THE ASTROPHYSICAL JOURNAL, 356:62–74, 1990 June 10

INFRARED STUDIES OF ELLIPTICAL GALAXIES. II. A RADIO-SELECTED SAMPLE

C. D. IMPEY[1,2,3]
Steward Observatory, University of Arizona
AND
C. G. WYNN-WILLIAMS[1,2] AND E. E. BECKLIN[1,2]
Institute for Astronomy, University of Hawaii
Received 1989 August 7; accepted 1989 December 14

ABSTRACT

We have made an infrared survey of radio galaxies in the Bologna B2 catalog. We find that 40% of our sample have infrared luminosities of at least $10^9\ L_{\odot}$, as opposed to about 8% of normal ellipticals. The galaxies are inhomogeneous in their infrared properties; some galaxies have active nuclei, while others appear to be powered by star formation. The most infrared-luminous galaxies in our sample are those listed as "peculiar" by Zwicky. Statistically, these galaxies are strikingly different from Seyfert galaxies in their infrared properties in that they show much more radio emission in comparison with their infrared emission than do Seyferts, even when the emission from the extended radio lobes has been discounted.

We also reanalyze the available data on the infrared properties of normal elliptical galaxies and find confirmation that the 10–12 μm emission from these galaxies comes either from circumstellar dust shells around evolved stars or from PAH-like (polycyclic aromatic hydrocarbon) grains.

Subject headings: galaxies: photometry — infrared: sources — radio sources: galaxies

I. INTRODUCTION

Elliptical galaxies are generally much weaker infrared sources than spirals. Several recent studies, however, have been successful in detecting substantial quantities of 2–100 μm emission from a number of early-type galaxies. During a ground-based 10 μm survey with the IRTF, the present authors (Impey, Wynn-Williams, and Becklin 1986, hereafter Paper I) detected 23 out of 65 elliptical galaxies selected mainly from the Shapley-Ames catalog. We suggested in that paper that the 10 μm emission arises mainly from the circumstellar dust shells of stars undergoing mass loss. Jura *et al.* (1987) studied the far-infrared emission from a similar, though not identical, sample by "addscanning" data from the *IRAS* survey. They detected 100 μm emission from about half their sample and attributed it to the presence of cold dust in the interstellar medium of the galaxies. The 100 μm emission detected by Jura *et al.* has a quite different color temperature from the 10 μm emission described by Impey, Wynn-Williams, and Becklin, so the different explanations put forward by the two groups are not necessarily in any conflict. Other *IRAS*-based studies of early-type galaxies include those of Bally and Thronson (1989) and Walsh *et al.* (1989).

Infrared emission has also been detected from some elliptical galaxies that show signs of nuclear activity at other wavelengths, but there is no consensus about its interpretation. Puschell (1981) observed six radio galaxies at 10 μm and concluded that their infrared excesses were due to dust emission in the nucleus. However, Heckman *et al.* (1983) studied the nuclei of 43 bright ($m_v < 18$) galaxies with $S_{5\,\mathrm{GHz}} > 0.20$ Jy and in 85% of the cases found a nonstellar optical/infrared continuum that had a strength roughly proportional to that of the compact radio source. At longer wavelengths Wrobel, Neugebauer, and Miley (1986) have studied 10 optically bright ellipticals with compact, nonthermal radio cores using the *IRAS* data base. Since the far-infrared emission in four cases is not a smooth extrapolation of the radio core spectrum, they conclude that the far-infrared emission is of nonthermal origin. The difficulty of deciding between thermal and nonthermal emission mechanisms for the infrared emission is illustrated by NGC 1052 (Becklin, Tokunaga, and Wynn-Williams 1982; Rieke, Lebofsky and Kemp 1982). NGC 1052 has a variable, compact radio source, nuclear emission lines, significant linear polarization, and a strong infrared excess. However, the 10 μm flux does not vary significantly (Paper I), and the infrared slope is steeper than that of most quasars or blazars. Both synchrotron emission and cool dust emission may contribute to the infrared power of this active galaxy.

In this paper, we present ground-based and *IRAS* "addscan" observations of a complete sample of nonspiral galaxies that have been selected on the basis of their radio continuum emission.

II. THE SAMPLE

The galaxies studied in this paper were selected by Colla *et al.* (1975*a*) from the Bologna B2 survey of 408 MHz radio sources. Identifications were made with galaxies in the Zwicky catalogs. Spiral galaxies were specifically omitted from this sample, leaving 54 ellipticals and three peculiar galaxies. The sample, which is sometimes known as the "B2 bright galaxy" sample, is listed in column (1) of Table 1. Other common names for the galaxies are given in column (2). Redshifts (col. [9]), identifications, and finding charts for the sources have been published by Colla *et al.* (1975*b*). Radio maps of these sources, made at Westerbork and the Very Large Array (VLA), have been published in a series of papers from the Bologna

[1] Visiting Astronomer, NASA Infrared Telescope Facility (IRTF), which is operated by the University of Hawaii under contract from the National Aeronautics and Space Administration.

[2] Visiting Astronomer, United Kingdom Infrared Telescope (UKIRT), which is operated by the Royal Observatory Edinburgh for the Science and Engineering Research Council.

[3] Guest Investigator, Infrared Processing and Analysis Center (IPAC), which is operated by the California Institute of Technology under contract from the National Aeronautics and Space Administration.

TABLE 1

10 to 100 Micron Data

B2 Name (1)	Other Name (2)	$S_{10\mu m}$[a] (3)	$S_{12\mu m}$ (4)	$S_{25\mu m}$ (5)	$S_{60\mu m}$ (6)	$S_{100\mu m}$ (7)	*IRAS* Data Type[b] (8)	z (9)	Log P_{408} W Hz^{-1} (10)	M_{pg} (11)	Log P_{ir} $L_{\odot}$ (12)	Core 21 cm Flux (mJy) (13)	Compactness[c] (%) (14)	Reference[d] (15)	Notes[e] (16)
0034+25	...	-4.8 ± 6.0	<103	<113	<153	<378	SC	0.0321	23.73	-19.6	<9.98	5.4	4	FFdRP87	...
0055+30	NGC 315	18.5 ± 7.2*	79 ± 10	125 ± 13	363 ± 17	586 ± 47	AO	0.0167	24.17	-20.6	9.71	420	23	BDFWS79	1
0055+26	NGC 326	-1.8 ± 6.0	<40	<67	<64	<170	AO	0.0472	25.32	-20.4	<9.96	<30	<2	EFLP78	2,3
0104+32	3C 31	10.2 ± 7.5	<40	<67	444 ± 21	1720 ± 57	AO	0.0169	24.73	-19.5	10.00	45	1	FBWP80	1
0116+31	4C 31.04	9.5 ± 6.6	<40	<60	154 ± 21	539 ± 57	AO	0.0592	25.37	-20.2	10.60	2500	100	FFdRP87	1
0120+33	NGC 507	9.8 ± 5.7	<84	115 ± 31	200 ± 47	<347	SC	0.0164	23.55	-20.1	9.45	2	3	FFdRP87	...
0149+35	NGC 703	17.4 ± 7.0*	<30	<47	273 ± 17	1247 ± 56	AO	0.0160	23.25	-18.5	9.78	12.7	16	FFdRP87	...
0206+35	4C 35.03	-9.6 ± 6.6	<87	<86	<126	<284	SC	0.0375	25.09	-20.1	<10.02	128	6	FFdRP87	...
0207+38	NGC 828	74.9 ± 7.3*	750 ± 50	1030 ± 55	10870 ± 50	25670 ± 250	SC	0.0181	23.34	-20.4	11.33	111	...	FFdRP87	4
0222+36	...	13.3 ± 6.6*	<87	<93	<126	<315	SC	0.0327	23.84	-19.7	<9.92	187	92	FFdRP87	...
0258+35	NGC 1167	-7.9 ± 6.4	<91	<99	177 ± 47	<441	SC	0.0160	24.28	-19.2	9.44	1780	98	FFdRP87	...
0326+39	...	7.6 ± 6.3	<96	<106	<140	<410	SC	0.0243	24.33	-19.4	<9.74	70	5	EFLP81	2
0331+39	4C 39.12	21.2 ± 6.7*	<101	<113	<140	<410	SC	0.0202	24.13	-19.9	<9.58	222	25	FFdRP87	...
0648+27	...	120.9 ± 10.3*	199 ± 14	1015 ± 29	2758 ± 21	2419 ± 57	AO	0.0409	23.94	-20.7	11.29	152	100	FFdRP87	...
0722+30	...	-6.4 ± 9.4	139 ± 14	448 ± 25	3190 ± 21	5141 ± 57	AO	0.0191	23.42	-18.0	10.77	27	20	FFdRP87	...
0755+37	NGC 2484	0.9 ± 9.2	<94	<106	<140	<347	SC	0.0413	25.28	-20.1	<10.16	212	8	FFdRP87	1
0800+24	...	-12.9 ± 7.8	<96	<152	<140	<315	SC	0.0433	24.06	-19.4	<10.19	1	1	FFdRP87	...
0836+29	4C 29.30	31.0 ± 8.7*	67 ± 9	149 ± 18	487 ± 13	614 ± 38	AO	0.0650	25.10	-20.3	10.98	21	4	FFdRP87	...
0844+31	4C 31.32	-1.9 ± 8.3	<91	<126	<140	<315	SC	0.0675	25.51	-20.5	<10.57	25.1	2	FFdRP87	1
0910+35	...	0.9 ± 8.7	<96	<113	<126	<315	SC	0.0240	23.34	-18.3	<9.65	...	...	...	5
0915+32	...	0.4 ± 8.0	<101	<133	<140	<315	SC	0.0620	24.54	-20.3	<10.50	10.7	4	FFdRP87	...
0916+34	NGC 2823	1.2 ± 9.0	<91	<119	<135	<315	SC	0.0232	23.82	-18.0	<9.64	...	...	...	5
0924+30	...	9.0 ± 8.0	<94	<126	<126	<315	SC	0.0266	24.37	-19.4	<9.74	<2	<1	EFLP81	2
1040+31	...	9.0 ± 9.6	<136	<172	<195	<473	SC	0.0360	24.62	-19.0	<10.18	43	6	FFdRP87	...
1101+38	...	31.5 ± 9.2*	90 ± 15	95 ± 19	181 ± 22	361 ± 68	AO	0.0300	24.30	-21.0	9.95	518	96	FFdRP87	6
1102+30	...	1.2 ± 7.6	<91	<113	<140	<347	SC	0.0720	24.98	-20.3	<10.65	10	3	FFdRP87	...
1108+27	...	-6.5 ± 12.9	<110	<139	<153	<315	SC	0.0331	23.62	-19.7	<9.97	14	16	FFdRP87	...
1113+29	4C29.41	...	<103	<126	<153	<315	SC	0.0489	25.36	-20.1	<10.31	34	2	FFdRP87	...
1122+39	NGC 3665	18.8 ± 8.4*	105 ± 30	128 ± 33	1813 ± 47	7014 ± 116	SC	0.0067	22.40	-19.3	9.80	20	22	FFdRP87	7

TABLE 1—*Continued*

B2 Name (1)	Other Name (2)	$S_{10\mu m}$[a] (3)	$S_{12\mu m}$ (4)	$S_{25\mu m}$ (5)	$S_{60\mu m}$ (6)	$S_{100\mu m}$ (7)	*IRAS* Data Type[b] (8)	z (9)	Log P_{408} W Hz^{-1} (10)	M_{pg} (11)	Log P_{ir} $L_{\odot}$ (12)	Core 21 cm Flux (mJy) (13)	Compactness[c] (%) (14)	Reference[d] (15)	Notes[e] (16)
1144+35	...	...	...	...	...	...	...	0.0630	24.40	-20.1	...	568	95	FFdRP87	...
1217+29	NGC 4278	18.5 ± 8.4*	65 ± 13	112 ± 22	618 ± 21	2041 ± 57	AO	0.0021	21.69	-17.7	8.29	470	100	SFFP83	1,3
1254+27	NGC 4839	...	<110	<111	<149	<347	SC	0.0249	23.40	-20.0	<9.74	2.3	4	FFdRP87	...
1256+28	NGC 4889	...	<17	<27	<25	<85	AO	0.0224	24.15	-18.7	<8.96	<2	<1	OO85	1,2
1257+28	NGC 4874	...	<17	<27	<25	<85	AO	0.0239	23.74	-19.6	<9.01	<3	<2	FG85	2
1317+33	NGC 5098	...	<110	<104	<149	<347	SC	0.0379	23.82	-19.7	<10.10	11	14	FFdRP87	...
1318+34	ARP 193	178.0 ± 16.0*	360 ± 40	1420 ± 50	14780 ± 50	23680 ± 250	SC	0.0232	23.36	-18.7	11.60	84	89	FFdRP87	4
1321+31	NGC 5127	...	<101	<99	<140	<347	SC	0.0161	24.25	-19.0	<9.35	7.7	0	FLPBEF82	...
1322+36	NGC 5141	...	<101	<93	<153	<378	SC	0.0175	24.00	-19.0	<9.46	73	9	FFdRP87	...
1346+26	4C 26.42	...	<40	<53	<64	<170	AO	0.0633	25.38	-20.3	<10.21	53.5	5	vBHM84	...
1350+31	3C 293	31.0 ± 11.0*	<37	<53	239 ± 21	643 ± 57	AO	0.0452	25.60	-19.4	10.49	3750	80	BFC81	1
1401+35	NGC 5444	...	122 ± 30	<92	<140	<336	SC	0.0133	23.80	-19.6	<9.17	...	...	...	5
1422+26	...	...	<119	<80	<140	<315	SC	0.0370	24.72	-19.0	<10.05	12	2	FFdRP87	...
1506+34	...	...	<110	270 ± 40	2570 ± 50	5030 ± 50	SC	0.0452	24.01	-19.4	11.46	115	91	FFdRP86	4,8
1525+29	...	-2.3 ± 7.2	<90	<80	<126	<284	SC	0.0653	24.55	-20.5	<10.50	20	9	FFdRP86	2
1553+24	...	-2.1 ± 6.1	<84	<80	<126	<294	SC	0.0426	23.84	-19.5	<10.13	53	43	FFdRP87	...
1602+34	...	9.7 ± 7.7	<83	<75	353 ± 42	1218 ± 84	SC	0.0316	23.68	-19.0	10.41	...		...	... 5
1610+29	NGC 6086	-7.3 ± 10.8	<77	<73	<126	<284	SC	0.0313	23.78	-19.5	<9.86	<1	<1	PdRFF86	...
1615+35	NGC 6109	8.3 ± 7.8	<77	<73	<112	<284	SC	0.0296	24.96	-19.1	<9.78	200	10	EFLP78	1,2
1621+38	NGC 6137	11.8 ± 10.5	<77	<73	<126	<284	SC	0.0310	24.23	-20.2	<9.85	31	8	FFdRP87	...
1626+39	NGC 6166	7.7 ± 10.5	<20	<27	<38	<113	AO	0.0303	25.50	-20.5	<9.37	146	4	FFdRP87	...
1652+39	Mrk 501	29.5 ± 6.7*	39 ± 4	67 ± 4	107 ± 9	<400	AO	0.0337	24.59	-20.8	9.66	1382	100	FFdRP87	6
1833+32	3C 382	57.5 ± 6.6*	72 ± 4	96 ± 4	98 ± 9	<300	AO	0.0586	25.95	-20.4	10.15	194	6	FFdRP87	...
1855+37	...	-9.2 ± 6.9	<87	<73	<112	<315	SC	0.0552	24.67	-21.2	<10.35	54	20	FFdRP87	...
2116+26	NGC 7052	6.9 ± 6.6	54 ± 10	47 ± 13	538 ± 17	1276 ± 57	AO	0.0164	23.22	-19.4	9.94	42	40	FFdRP87	...
2229+39	3C 449	21.6 ± 6.3*	<91	<86	186 ± 42	1029 ± 137	SC	0.0181	24.61	-19.1	9.78	19	1	PWS79	1
2236+26	...	-2.8 ± 6.6	<98	<93	<140	<347	SC	0.0277	24.05	-19.3	<9.82	6.7	2	FFdRP87	...
2335+26	NGC 7720	-10.6 ± 8.3	<40	<54	149 ± 21	<198	AO	0.0301	25.54	-20.4	9.80	150	2	EBOO84	1,2

[a] * = 2σ detection at 10 μm.

[b] AO = *IRAS* pointed observation; SC = survey co-added.

[c] The ratio of the 21 cm core flux to the total 21 cm emission.

[d] References: BDFWS79: Bridle *et al.* 1979; BFC81: Bridle, Fomalont, and Cornwell 1981; EBOO84: Eilek *et al.* 1984; EFLP78: Ekers *et al.* 1978; EFLP81: Ekers *et al.* 1981; FBWP80: Fomalont *et al.* 1980; FFdRP86: Fanti *et al.* 1986; FFdRP87: Fanti *et al.*, 1987; FG85: Feretti and Giovannini 1985; FLPBEF82: Fanti *et al.* 1982; OO85: O'Dea and Owen 1985; PdRF86: Parma *et al.* 1986; PWS79: Perley, Willis, and Scott 1979; SFFP83: Schilizzi *et al.* 1983; vBHM84: Van Breugel, Heckman, and Miley 1984.

[e] Notes: 1 = total 21 cm flux from Colla *et al.* 1975*b*; 2 = core flux density estimated from map; 3 = structure information based on 6 cm data; 4 = peculiar galaxy; 5 = probable misidentification; 6 = BL Lac object; 7 = dust lane; 8 = possible misidentification.

group; we have drawn extensively on the summary of this work contained in Fanti *et al.* (1987). Because the optical identifications are based on the Zwicky catalog, the galaxies are brighter than 15.7 mag. Consequently the galaxies in this sample are much closer (median distance of 120 Mpc, assuming $H_0 = 75$ km s^{-1} Mpc^{-1}) than most of those in, say, the 3C catalog. They therefore generally have comparatively low radio luminosities; the median 408 MHz luminosity is about 1.5×10^{24} W Hz^{-1}—a factor of 20 lower than that of the sample selected by Golombek, Miley, and Neugebauer (1988).

After we had undertaken the major part of our observational program, Fanti *et al.* (1987) reconsidered some of the identifications on which the sample is based. They suggested that 0910+35, 0916+34, 1401+35, 1506+34, and 1602+34 are likely to have been misidentified. We have flagged four of these sources in Table 1 but, as we shall argue in § V*d*, the very strong 60 μm emission detected from the direction of 1506+34 provides strong circumstantial evidence that the original optical identification of the radio galaxy was correct. We have therefore given it the benefit of the doubt and included it in our discussions.

III. OBSERVATIONS

Ground-based measurements were obtained for 45 out of the 57 radio sources at 10 μm. Of these, 12 were also observed in the 1–4 μm region. Twelve sources in the R.A. range 11^h–15^h were not observed due to the constraints of telescope scheduling. *IRAS* co-added survey or pointed observations were obtained for 56 galaxies; one galaxy lies in a region of the sky having no survey data.

a) Ground-based 10 μm *Observations*

All the 10 μm ground-based data for this paper were obtained at the 3 m NASA Infrared Telescope Facility (IRTF) on Mauna Kea. A gallium-doped germanium bolometer was used at the Cassegrain focus with a 5".7 circular entrance aperture, a 10" or 20" chopper spacing, and a broad-band 8–13 μm filter. A total integration time of 20 minutes per galaxy yielded an average noise sensitivity of 7.9 mJy, making this experiment roughly 8 times more sensitive than the *IRAS* survey in the 12 μm band. The 45 galaxies were measured on 10 separate nights during 1982 September, 1983 January, February, March, and September, and 1988 January. The observing technique, calibration, and data reduction are exactly the same as described in Paper I.

The 10 μm flux densities and errors are listed in column (3) of Table 1. Galaxies having a flux density with significance greater than 2 σ are marked with an asterisk in column (3). The flux densities have not been corrected for the bandwidth of the 10 μm filter; this effect is at most 10%. No extinction corrections have been applied, since they would be much smaller than the statistical errors. No bias is introduced by neglecting an extinction correction, since standards and objects were observed at very similar air masses.

b) Ground-based 1–4 μm *Observations*

To supplement the 10 μm data, we obtained 1–4 μm photometry of 12 galaxies, including most of the strong 10 μm sources in the sample. An indium antimonide (InSb) detector cooled by solid nitrogen was used at the Cassegrain foci of both IRTF and the 3.8 m United Kingdom Infrared Telescope (UKIRT) on Mauna Kea. The data were acquired during the periods 1983 September 2–6 (IRTF) and 1984 March 23–26 (UKIRT). The apertures used were 5".8 (IRTF) and 7".5 (UKIRT) in diameter, but identical standard *JHKL'* filters were used at the two telescopes. More details of the observing and calibration procedure may be found in Paper I.

Table 2 gives the details of the near-infrared data, with the B2 galaxy name and the ratio of aperture size to galaxy diameter, log *A*/*D*(0), in columns (1) and (2), respectively. Following the units of de Vaucouleurs, de Vaucouleurs, and Corwin (1976), log *A*/*D*(0) is the decimal logarithm of the ratio of the aperture to the effective diameter in units of 0'.1. The galaxy magnitudes at *J*, *H*, *K*, and *L'*, corrected only for the atmospheric extinction, are given in columns (3), (5), (7), and (9). The colors in columns (4), (6), and (8) have been corrected for a series of effects that are described in detail in Paper I. The telescope used is given in column (10).

c) IRAS Data

All but one of the B2 ellipticals are in regions of the sky surveyed by the *IRAS* satellite. Ten have fluxes listed in the *IRAS Point Source Catalog, Version 2* (1988), but only five are detected in more than two bands, and only one is detected in all four bands. Substantial gains in sensitivity are possible

TABLE 2

NEAR-INFRARED DATA[a]

Galaxy (1)	log $A/D(0)$[b] (2)	J (3)	$J-H$ (4)	H (5)	$H-K$ (6)	K (7)	$K-L'$ (8)	L' (9)	Telescope (10)
0055+30	−1.26	12.05	(0.70)	11.16	(0.19)	10.92	(0.39)	10.54	IRTF
0149+35	−1.30	13.11	(0.75)	12.19	(0.19)	11.95	(0.19)	11.77	IRTF
0207+38	−1.23	12.31	(0.85)	11.27	(0.36)	10.84	(0.69)	10.17	IRTF
0331+39	−1.35	12.01	(0.68)	11.11	(0.20)	10.83	(0.32)	10.44	IRTF
0648+27	−1.00	12.89	(0.65)	12.03	(0.33)	11.54	(1.68)	9.87	IRTF
1101+38	−1.10	10.81	(0.60)	10.35	(0.56)	9.74	(1.29)	8.80	UKIRT
1217+29	−1.43	10.36	(0.73)	9.58	(0.20)	9.38	(0.28)	9.10	UKIRT
1652+39	−1.05	11.62	(0.75)	11.02	(0.43)	10.55	(1.00)	9.82	UKIRT
1833+32	−0.80	13.02	(0.72)	12.07	(0.56)	11.29	(1.68)	10.96	IRTF
1855+37	−0.75	13.04	(0.59)	12.27	(0.23)	11.84	(0.30)	11.54	UKIRT
2116+26	−1.40	11.77	(0.59)	11.00	(0.33)	10.61	(0.33)	10.25	UKIRT
2229+39	−1.23	12.68	(0.74)	11.73	(0.21)	11.43	(0.28)	11.16	IRTF

[a] Colors include various corrections discussed in § III*b*. Zero magnitude at *J*, *H*, *K*, and *L'* corresponds to 1600, 1020, 657, and 252 Jy, respectively.

[b] Values of log *A*/*D*(0) from de Vaucouleurs, de Vaucouleurs, and Corwin 1976.

using either the co-addition of the survey data base (a factor of 3) or additional pointed observations where available (a factor of up to 5). The analysis was carried out at the Infrared Processing and Analysis Center (IPAC) in Pasadena. Pointed observations were available for 19 galaxies. The survey was co-added in 0°5 × 1°0 fields for the remaining 37 galaxies. Table 1 lists the *IRAS* flux densities or 3 σ upper limits in mJy. Columns (4), (5), (6), and (7) give the flux densities and errors in band 1 (12 μm), band 2 (25 μm), band 3 (60 μm), and band 4 (100 μm), respectively. Column (8) denotes the type of data, "AO" for pointed observation and "SC" for survey co-add. Color corrections to the flux densities are based on an assumed $S_\nu \propto \nu^{-1}$ flux distribution. These corrections and general comments about the accuracy and reliability of *IRAS* data are contained in the *IRAS Explanatory Supplement* (1988) and the guide to pointed observations by Young *et al.* (1988).

IV. RESULTS

a) *Detections at* 10 μm

We detected one-third of our sample (15/45) at 10 μm with a significance of 2 σ or greater; they are marked with an asterisk in Table 1. Strictly speaking, however, for statistical purposes our success rate should be considered to be 12/42, since the three galaxies we observed in 1988 February (namely 1122+39, 1318+34, and 1350+31) were looked at with the knowledge that they had been detected by *IRAS* at at least two wavelengths. On the other hand, three of our nondetections (0910+35, 0916+34, and 1602+34) are now considered misidentifications by Fanti *et al.* (1987), bringing our detection rate back to 12/39.

We have made estimates of the significance of these detections using three statistical tests, namely the Mann-Whitney U-test, the $P(\geq S_0)$ statistic, and the Lucy deconvolution algorithm. These tests, and their application to our 10 μm photometry, are described in some detail in Paper I, as are the results of tests we made to check that observations of blank pieces of sky led to no significant detections. As it happens, the detection rate in the present paper is very similar to that in Paper I, and the statistical analyses lead to the same conclusion, namely that almost all the 2 σ detections may be considered to be real.

b) *IRAS Detections*

Of the 56 galaxies in our sample that were observed by *IRAS*, 23 were detected at at least one wavelength (see Table 1). The mean discrepancy between the *IRAS* and the central radio source positions was 34″. Twenty-four galaxies on our list were independently analyzed by Golombek, Miley, and Neugebauer (1988). On the whole, the agreement is satisfactory, given the need for some judgment in the face of the non-Gaussian baseline uncertainties inherent in the flux determination of faint sources. The most significant differences are that we count 0149+35 and 0258+35 as detections at 60 μm, but Golombek, Miley, and Neugebauer do not. Both detections are marginal; 0149+35 has a larger than average (79″) position discrepancy, while 0258+35 is a low signal-to-noise detection. Nineteen of our galaxies were included in a survey of Knapp *et al.* (1989). Agreement between our results and those of Knapp *et al.* is less good than with Golombek, Miley, and Neugebauer. In most cases, the differences are probably due to different criteria adopted for positional identification, strong cirrus, or poor signal-to-noise.

A possible problem with identifying *IRAS* emission with particular galaxies is that emission may arise from dust-rich companions to the radio galaxy. We examined visible-wave images of all the galaxies. The only possible complications arise in the cases of 0116+31, for which the optical counterpart of the radio source has a small bluer companion only 0′4 away (van den Bergh 1970); 0104+32, which may be associated with a pair of galaxies; and 0149+35, which is in a cluster, and whose identification has already been discussed in this section.

c) *Energy Distributions*

In Figure 1 we combine our ground-based and *IRAS* data to plot energy distributions of all galaxies with detections at more than one infrared wavelength. Some previously published 1–4 μm data are also included. We also show the total radio emission from the galaxies; emission from both the galaxy itself and from the extended lobes is included in these graphs. Note that the 1–10 μm data were obtained using a beam with a diameter less than 10% of that used for the 12–100 μm data.

Almost all galaxies we detected have a 12–100 μm energy distribution that increases monotonically with wavelength. The only significant exception is 1401+35, which is the only source detected at 12 μm but not at 60 μm. This galaxy is now considered a misidentification by Fanti *et al.* (1987), implying that the galaxy does not contain a radio source; since the galaxy is very bright at visible wavelengths, what we are detecting is probably emission from circumstellar dust shells of stars, as in the galaxies discussed in Paper I.

Most of the galaxies we observed in the 1–4 μm range show a clear secondary flux density maximum near 1.65 μm. This peak can be attributed to the emission from the late-type stellar population in these galaxies. In most cases, short-wavelength extrapolation of the radio emission lies well below the level of infrared emission. This behavior contrasts with that of most quasars and blazars, including the two known BL Lac objects in our sample, 1101+38 and 1652+39.

d) *Global Properties*

Table 1 includes some global properties for the galaxies. The redshifts (col. [9]), monochromatic 408 MHz luminosity (col. [10]), and absolute photographic magnitudes (col. [11]) are taken from Colla *et al.* (1975*b*), adjusted for a Hubble constant of 75 km s^{-1} Mpc^{-1}. The far-infrared luminosity (expressed as a decimal logarithm of solar units in col. [12]) is derived from the 60 and 100 μm flux densities using the formulae suggested in the *Cataloged Galaxies in the IRAS Survey, Version 2* (1989).

V. DISCUSSION

a) *Comparison with Other Samples*

The median distance of the galaxies in this radio selected sample is about 5 times that of the optically selected galaxies in Paper I. Since the detection rate for the two samples is almost the same, we can draw the immediate conclusion that the presence of a radio source in an elliptical galaxy increases the probability that it emits strong 10 μm emission from its nuclear region.

The detection rate by *IRAS* is slightly lower than that of the Jura *et al.* (1987) survey of Shapley-Ames galaxies, but not by as much as would be expected given the much greater distance of the present sample. At least 40% of the entire sample have

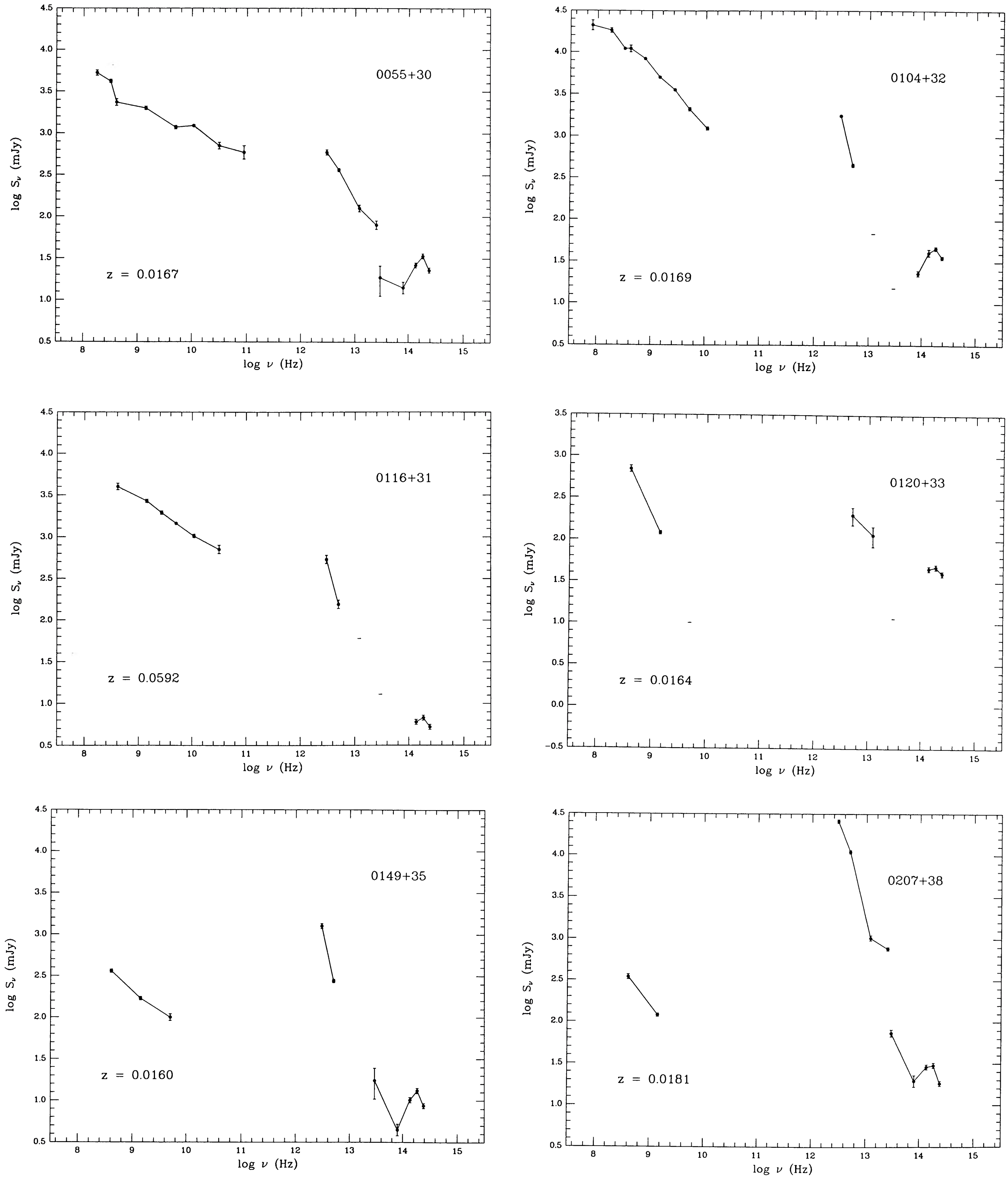

FIG. 1.—Energy distributions of sample galaxies. Data from 12–100 μm ($12.5 < \log \nu < 13.4$) are from *IRAS*. Data at 10 μm ($\log \nu = 13.47$) are from the IRTF (Table 1). Data from 1–4 μm ($\log \nu > 13.5$) come from Table 2 and from Gezari, Schmitz, and Mead (1987), Heckman *et al.* (1983), Lilly, Longair, and Miller (1985), and Elvis *et al.* (1984). Radio data refer to the total flux density of the sources and come from Colla *et al.* (1975*b*) and Kuhr *et al.* (1981). Upper limits are represented by small horizontal lines.

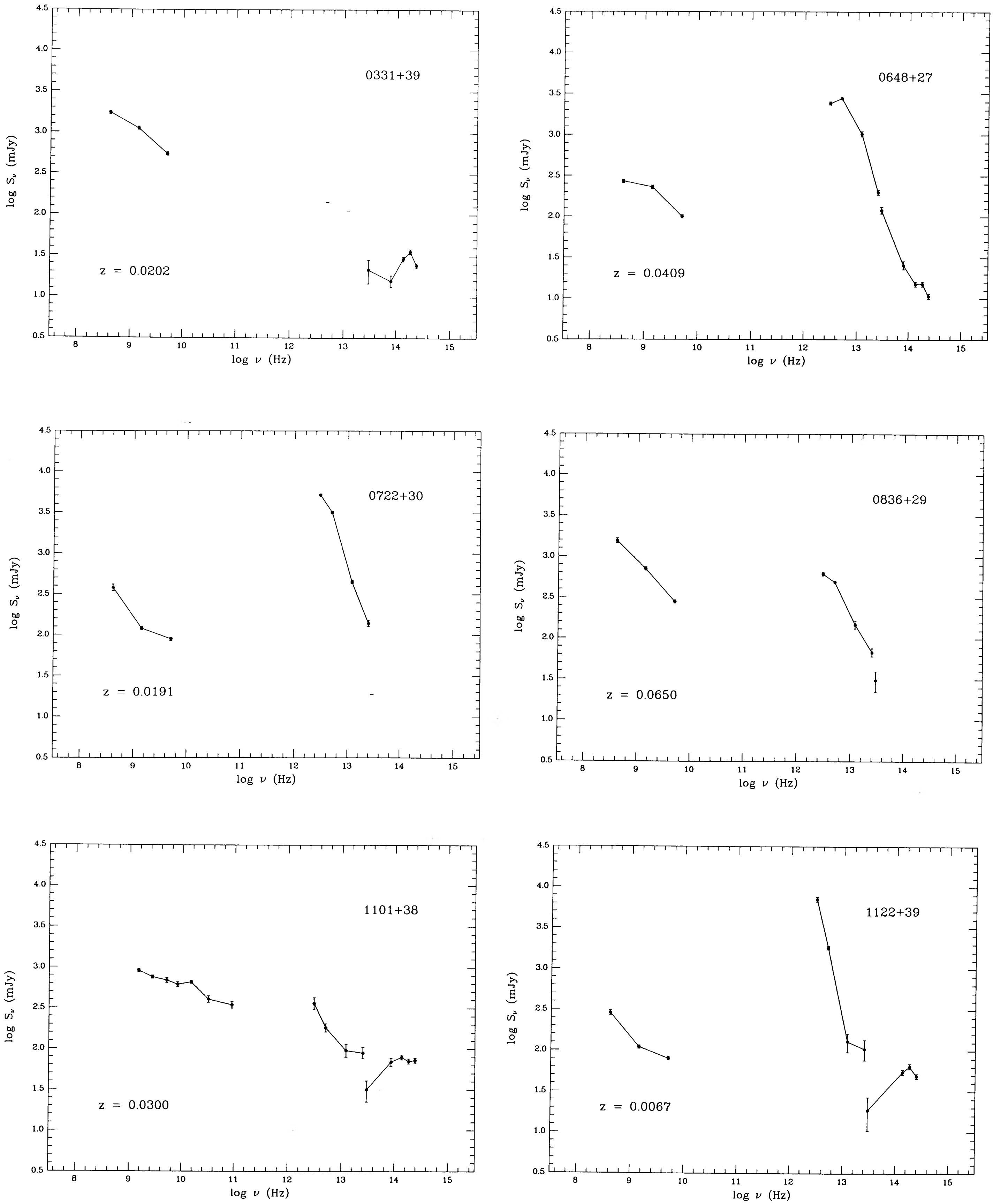

FIG. 1—*Continued*

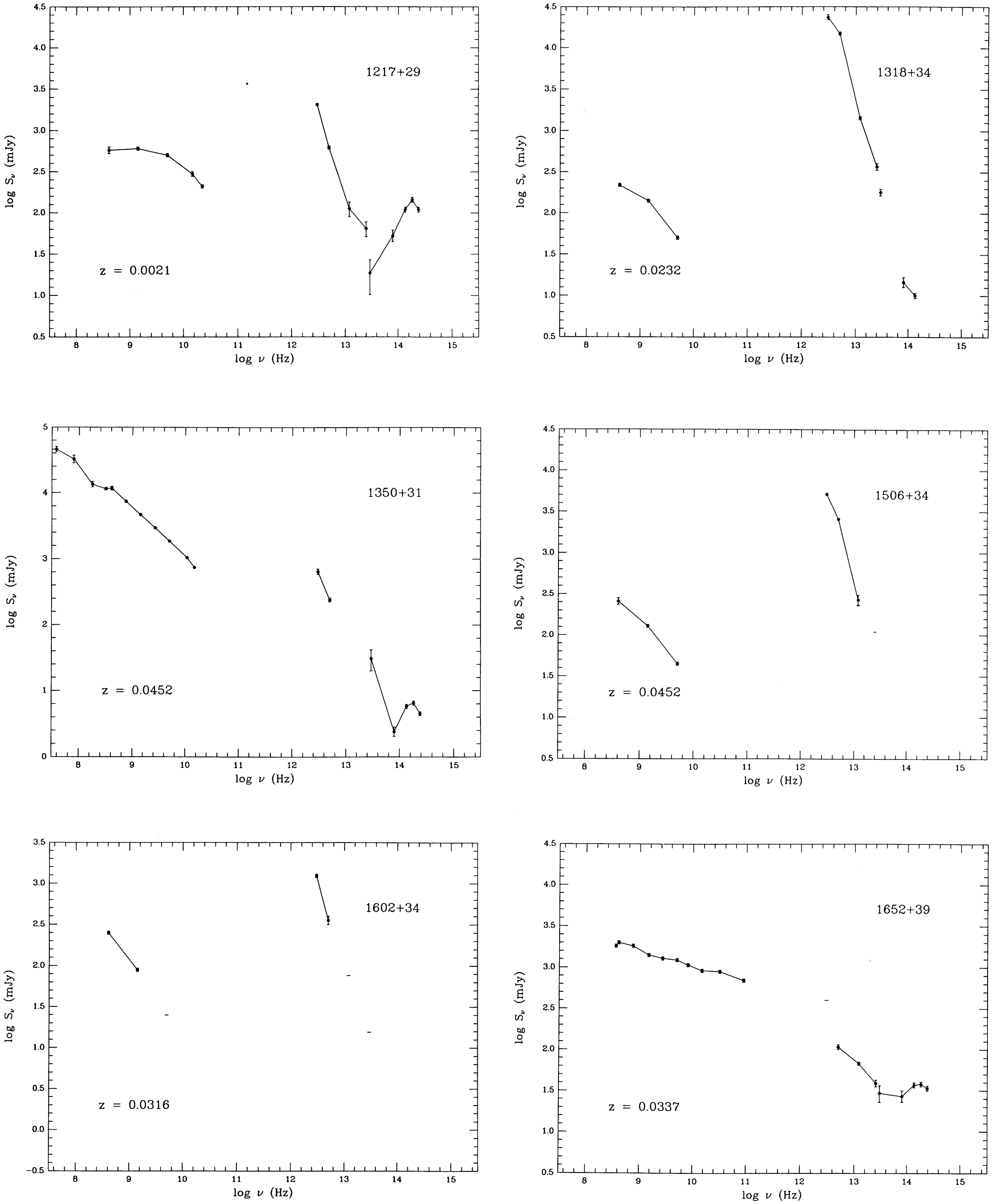

FIG. 1—*Continued*

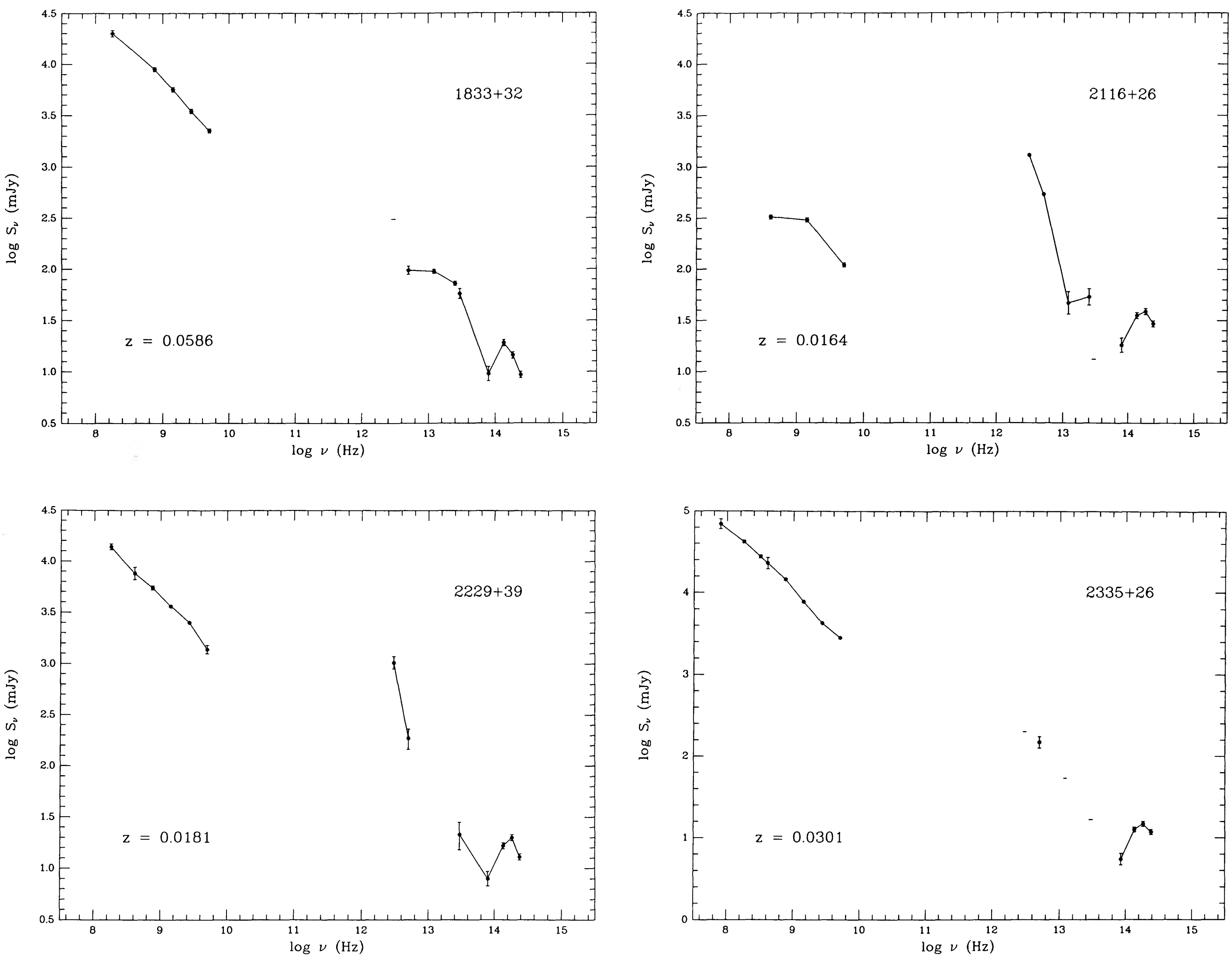

FIG. 1—*Continued*

$L_{ir} > 10^9\ L_\odot$. Only one galaxy is known to have a luminosity below $10^9\ L_\odot$. The high luminosities are of course due to the large distances of the galaxies, but the high detection rate is interesting when compared with detection rates for normal ellipticals. Jura (1986) studied early-type galaxies in the Shapley-Ames catalog and found only 10 out of 130 (8%) with $L_{ir} > 10^9\ L_\odot$. However, the proper comparison is with a volume-limited sample; Rieke and Lebofsky (1986) found only 4% of ellipticals from the unbiased *IRAS* sample to have $L_{ir} > 10^9\ L_\odot$. *It thus appears that radio galaxies are 10 times as likely to have strong infrared emission as are normal ellipticals.*

b) *Correlation with Radio Emission*

Although we have established (§ V*a*) that the presence of a radio source in a galaxy increases the likelihood that it emits strong infrared emission, when we looked at the galaxies *within* our sample we were unable to find any statistically significant relationships between their infrared properties and their *total* radio flux densities. We therefore focused our attention on that part of the radio emission that is associated with the central regions of these galaxies. As is demonstrated by the VLA studies summarized by Fanti *et al.* (1987), the total flux density of these radio sources is usually dominated by the emission from large-scale radio lobes that extend well beyond the confines of the optical galaxy. In almost all cases, however, there is an identifiable compact (< 5″) radio source at the center of the galaxy; in the BL Lac objects and a few other sources, this central source dominates. For most galaxies in the sample Fanti *et al.*, or other authors cited by them, give the 21 cm flux density of the source that coincides with the nucleus. We refer to this as the "core 21 cm flux" in column (13) of Table 1. In column (14) we list the "compactness" of the radio source, which we define as the ratio of the 21 cm core flux to the total 21 cm emission, including the radio lobes. A point source would have a compactness of 100%. In column (15) we provide a reference to the paper from which the structural information is derived.

Graphs of 60 and 10 μm flux densities as a function of 21 cm core flux density are presented in Figures 2 and 3, with different symbols used for the sources with radio compactness of

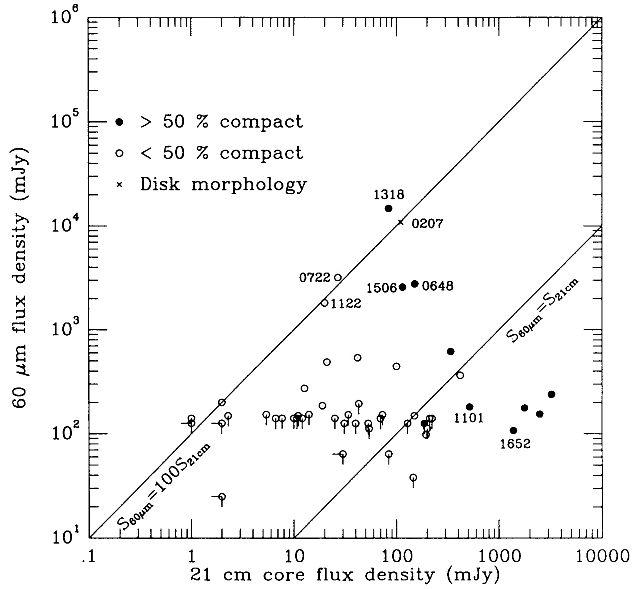

FIG. 2.—Core 21 cm flux density vs. 60 μm flux density for galaxies in the sample.

greater than or less than 50%. One galaxy, 0207+38, has a disklike radio morphology from which a compactness could not be determined. At first glance, the relationship between radio and infrared emission is weak; only one galaxy (1217+29—by far the closest and least luminous in the sample) lies in the top 20 percentile of both 60 μm and 21 cm flux densities. As we shall discuss in § V*e*, this lack of obvious correlation is in marked contrast to that found for most other samples of galaxies. To look for more subtle connections, we used the Kolmogoroff-Smirnoff (K-S) test to determine whether the infrared and radio flux densities are related to each other. First we sorted the 52 galaxies in our complete sample that were observed by *IRAS* into four bins according to their 21 cm core radio flux densities. The bins covered the categories of less than 10, 10–100, 100–1000, and greater than 1000 mJy. We then counted the number of galaxies in each bin that were detected at 60 μm. Application of the K-S test indicated that the distributions of 60 μm detections and nondetections were different at the 10% level, suggesting that the 60 μm and 21 cm core flux densities *are* marginally related to each other. A similar analysis of the 42 galaxies observed at 10 μm did *not* show any significant correlation between the 10 μm and 21 cm core flux densities.

The strongest links we found were between the compactness of the radio source and its probability of detection at 60 and 10 μm. The sense of the link is obvious from Figures 4 and 5—namely, that a radio galaxy that has more than 50% of its flux in the core is more likely to be detected at infrared wavelengths than one that is less centrally concentrated. The correlation is significant at the 1% level at 60 μm and at the 10% level at 10 μm. There is a potential selection effect that we should note here. Since the B2 survey is selected by *total* (core plus lobes) radio flux density, low–flux density/low-compactness cores are preferentially selected over low–flux density/high-compactness ones. High-compactness galaxies are therefore likely to be closer than low-compactness ones. This effect does not seem to be significant in practice, since the mean redshift of the 11 most compact galaxies is within 5% of the mean of the whole sample.

In Figure 2 we have plotted two diagonal lines that indicate at a glance the relative strengths of the radio and 60 μm emission from the galaxies, albeit measured at very different spatial resolutions. It shows that the ratio of infrared to radio flux varies from about 0.1 to about 100 for different galaxies. The differences are striking enough that we need to discuss the different groups of galaxies separately.

c) Galaxies with Low Infrared/Radio Flux Ratios

The galaxies with the lowest values of 60 μm to radio emission lie in the lower right-hand corner of Figure 2. Two features are of interest about these galaxies. First, the four galaxies with the largest 60 μm radio flux ratio all have a radio

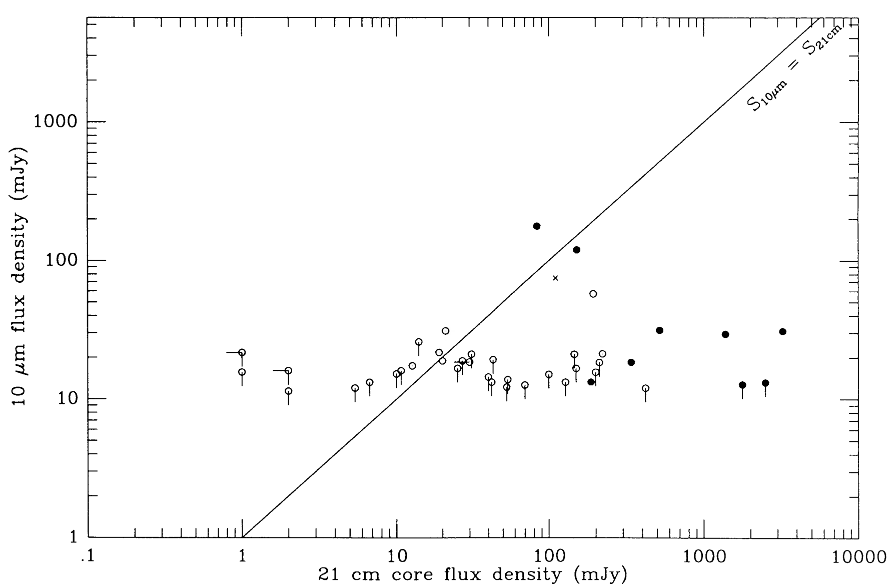

FIG. 3.—Same as Fig. 2 at 10 μm.

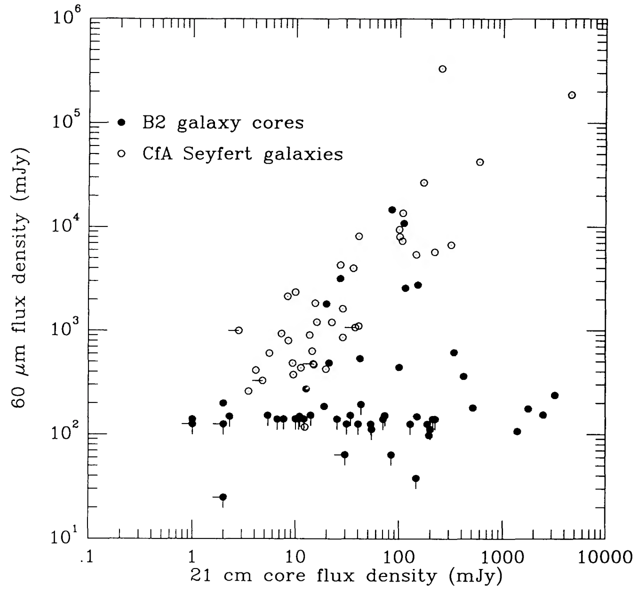

FIG. 4.—Same as Fig. 2, with Seyfert galaxies plotted for comparison.

compactness greater than 0.5. Second, both of the known BL Lac objects in the sample, namely 1101+38 and 1652+39, lie in the lower right-hand corner of the figure. As we will discuss further in § V*f*, the infrared energy distributions of these galaxies (Fig. 1) are flatter than those of most infrared galaxies. In these galaxies, the infrared emission is likely to be predominantly nonthermal (Impey and Neugebauer 1988). Although the 10 μm data are sparser, the same group of galaxies is seen in the lower right-hand corner of Figure 3.

d) *Galaxies with High Infrared/Radio Flux Ratios*

The galaxies with the highest infrared flux densities in our sample have 60 μm flux densities about 100 times the nuclear radio flux density. The similarity of this ratio to that typically found in spiral galaxies (Helou, Soifer, and Rowan-Robinson 1985; Wunderlich, Klein, and Wielebinski 1987) suggests that a similar combination of physical processes is taking place and that heated dust is responsible for the emission from the galaxies at 60 μm. There is some circumstantial evidence to

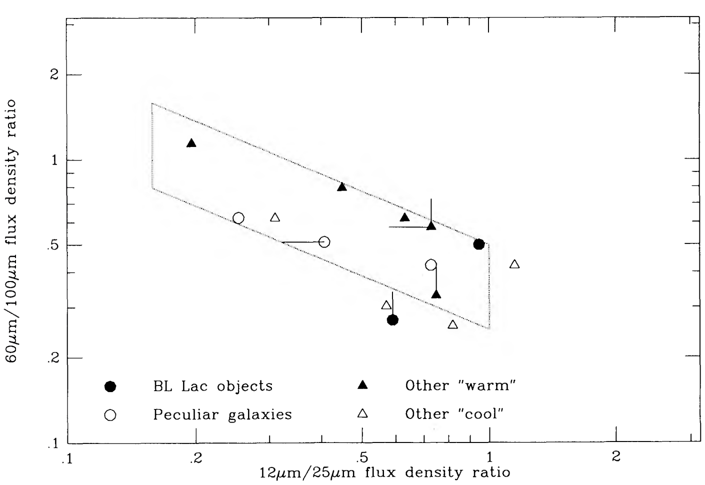

FIG. 5.—Color-color diagram for galaxies in the sample. The box shows the region of the diagram usually occupied by spiral galaxies. The words "warm" and "cool" refer to the 60 μm/25 μm color temperature (see § V*f*).

support this idea; the four bright galaxies closest to the $S_{60\,\mu m} = 100 S_{21\,cm}$ line all show evidence for nonellipsoidal components. Specifically, 0207+38 and 1318+34 are categorized as "peculiar" by Colla *et al.* (1975*b*), 1122+29 has a dust lane (Parma *et al.* 1986), and 0722+30 is an S0 system (Colla *et al.* 1975*b*). An even stronger link between infrared emission and optical morphology is that *the three most infrared-luminous galaxies in our sample are the three galaxies listed as "peculiar" by Zwicky.* These are 0207+38 (NGC 828), 1318+34 (Arp 193), and 1506+34. It is quite likely that the emission we are seeing arises from starbursts in these galaxies, as in the case with the Centaurus A radio galaxy, NGC 5128 (Joy *et al.* 1988; Marston and Dickens 1988).

In § II we noted that there was some uncertainty about the identification of 1506+34. Although we have no *direct* evidence (such as improved positions) with which to address this question, we point out that the detection of 2.5 Jy of 60 μm emission from this direction is very strong indirect evidence that the identification is correct. Given the rarity of unidentifiable extragalactic *IRAS* sources, it would be most remarkable if the 2.5 Jy did not come from the visible galaxy. It would also be remarkable if the radio emission came from anywhere but the direction of the *IRAS* source, since if there were no radio emission from 1506+34, its location in Figure 2 would move well to the left of the $S_{60\,\mu m} = S_{21\,cm}$ line—a region of the diagram that is otherwise devoid of galaxies.

e) *Comparison with Seyfert Galaxies*

Figure 4 shows a comparison of the galaxies in our sample and the Seyfert galaxies in the CfA sample studied by Edelson (1987) and Edelson, Malkan, and Rieke (1987). We have plotted total 21 cm flux densities for the Seyfert galaxies because the spatial extent of their radio emission never exceeds a few kpc (e.g., Ulvestad and Wilson 1984). As has been remarked on by several other authors, there is a linear relationship between radio and infrared emission for Seyfert galaxies that is very similar to that seen in spirals. There is clearly a major difference between the Seyfert and the B2 galaxies, in that there are no Seyferts in which the radio emission exceeds, or even approaches, the strength of the 60 μm emission. In other words, with few exceptions, *radio galaxy nuclei show much more radio emission as compared to infrared emission than do Seyfert galaxies, even when the emission from the extended lobes has been discounted.* It is generally believed that most of the infrared emission from Seyfert galaxies is ultraviolet energy reradiated by dust. The relative absence of infrared power from radio galaxy nuclei implies either that their central engines produce radio power without ultraviolet power, that radio emission is somehow suppressed in Seyfert galaxies, or that there is too little dust in radio galaxies to absorb the nuclear ultraviolet radiation. While the last alternative is consistent with radio galaxies being generally associated with ellipticals rather than spirals, the data in this paper do not allow us to exclude the first two possibilities.

f) *Infrared Colors*

It has been shown by de Grijp *et al.* (1985) that Seyfert and other active galaxy nuclei tend to have higher 25 μm/60 μm flux density ratios than galaxies without active nuclei. In a later paper (de Grijp, Miley, and Lub 1987), they make use of the criterion $S_{25\,\mu m} > 0.27 S_{60\,\mu m}$ to classify galaxies as "warm" (i.e., likely to contain an active nucleus) as opposed to "cool" (i.e., unlikely to contain an active nucleus). There are 14 galaxies in our sample for which both 25 and 60 μm flux densities exist, and application of the de Grijp *et al.* criterion to these galaxies yields the following results:

1. Both of the known BL Lac objects (1101+38 and 1652+39) are "warm," as would be expected for active nuclei.

2. All three "peculiar" galaxies (0207+38, 1318+34, and 1506+34) are "cool," as would be expected for galaxies in which some kind of starburst is occurring.

3. Of the nine remaining galaxies, five are "warm" and four are "cool." The fraction of galaxies having "warm" 25 μm/60 μm colors is significantly higher than the 5% found for the unbiased sample of galaxies considered by de Grijp, Miley, and Lub (1987), leading to the unsurprising conclusion that active nuclei are more common in radio galaxies than in the general galaxy population.

4. All six "cool" galaxies lie above the $S_{60\ \mu m} = S_{21\ cm}$ line in Figure 2, while five out of the eight "warm" galaxies lie below it. This difference is in accordance with the discussions of the emission mechanisms in these galaxies in §§ Vc and Vd.

Figure 5 shows the connection between 12 μm/25 μm and 60 μm/100 μm colors for the 14 galaxies discussed in this section. The parallelogram shows the region of the diagram where most spiral galaxies are found (Helou 1986). S0 galaxies populate a similar region in the diagram (Bally and Thronson 1989). All the galaxies in our sample lie within or close to the parallelogram, with no obvious segregation by galaxy type or 25 μm/60 μm color. Helou (1986) has suggested that in the case of spiral galaxies, the diagonal represents a trend from quiescent, cirrus-dominated galaxies in the lower right to more active star-forming galaxies in the upper left. The fact that galaxies of such divergent types all follow the same trend suggests that one should be cautious in applying Helou's explanation to all types of galaxies.

g) Infrared Sizes

The ratio of the IRTF 10 μm to *IRAS* 12 μm flux densities provides a crude measure of the size of the infrared-emitting regions in these galaxies. For most observed galaxies, the ratio is less than unity, indicating that the emission region is moderately compact. The lowest ratio of 10 μm/12 μm flux is found in 0207 + 38, one of the peculiar galaxies. The radio map (Fanti *et al.* 1986) shows an extended disklike structure with a diameter of about 15″ (5 kpc); our results indicate that the infrared emission is extended on this scale.

According to the data in Table 1, the source 1101+38 has a 10 μm/12 μm ratio of 30% and is therefore apparently extended. However, since it has a flat nonthermal 12–100 μm energy distribution and is known to be a BL Lac object, we suspect that it varied in flux between the dates on which the *IRAS* and IRTF data were obtained and that the infrared radiation is nonthermal.

h) Radio Luminosities

Figure 6 shows the radio to infrared spectral index α_{RI} plotted against radio power at 408 MHz for two sets of radio galaxies: B2 galaxies from this paper and powerful (mostly 3CR) galaxies from Golombek, Miley, and Neugebauer. A value of 0.5 is assumed for q_0. The spectral index α_{RI} is based on the flux densities at 6 cm and 60 μm and has the sense that $S_\nu \propto \nu^a$. For all these objects $\alpha_{RI} > -1$, so the power per octave is dominated by infrared emission. In Figure 6, the relationship between α_{RI} and log L_{RAD} is given by

$$\alpha = \text{constant} - 0.25 \log L_{RAD} ,$$

with large scatter. Since $\nu_{IR} = 100\nu_{RAD}$, we can write

$$\log (L_{IR}/L_{RAD}) = 2\alpha ,$$

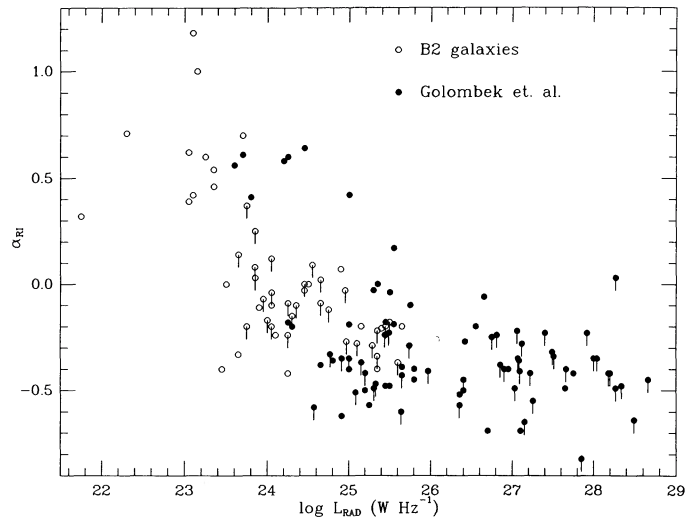

FIG. 6.—Relation between the radio-infrared spectral index α_{RI} and the radio luminosity for galaxies in this sample and in that of Golombek, Miley, and Neugebauer (1988).

from which we may deduce that $L_{IR} \propto (L_{RAD})^{0.5}$ and that the B2 and the higher luminosity radio galaxies of Golombek, Miley, and Neugebauer form a continuous single distribution. If it is true that powerful radio emission is associated with high levels of distributed star formation in the host galaxy, then the use of radio galaxies as standard candles for cosmology must be questioned.

From this complete sample of B2 galaxies we can estimate that the space density of radio galaxies with $L_{IR} \approx 10^9\ L_\odot$ is 2×10^{-5} Mpc^{-3}, it is interesting that this is similar to the space density of ultraluminous galaxies (Soifer *et al.* 1986).

i) Another Look at the Shapley-Ames Galaxies

The generally compact nature of the infrared sources in this sample is in contrast to that of the Shapley-Ames galaxies discussed in Paper I. With the publication of the "addscanned" *IRAS* data by Jura *et al.* (1987), it is now possible to estimate the infrared size of some of the galaxies in Paper I. There are eight galaxies for which there are both 10 μm detections in Paper I and 12 μm detections in Jura *et al.* (1987). Two of these galaxies, NGC 1052 and NGC 4278 (B2 1217+29) have well-established active nuclei that might vary. They have 10 μm/12 μm ratios of greater than 25%. All the other galaxies (NGC 221, 838, 4486, 4374, and 4698) have 10 μm/12 μm ratios between 0.08 and 0.14—smaller than almost all galaxies in the B2 sample. Part of the explanation for the difference is certainly that the B2 galaxies are farther away than the Shapley-Ames galaxies. Nevertheless, the low value of the 10 μm/12 μm flux ratio in Shapley-Ames ellipticals is an important result in itself, because it shows directly that the 10–12 μm emission in normal elliptical galaxies is extended, probably on the scale of the starlight itself. This result lends support to the suggestion in Paper I that the 10 μm emission arises from dust shells around evolved stars. Alternatively, it may arise in small PAH–like grains that are heated temporarily by stellar photons.

VI. CONCLUSIONS

The main conclusions of this paper are

1. Our detection rate for the radio galaxies in the B2 "bright" sample (median distance 120 Mpc) is 30% at 10 μm

and 40% at 60 μm. This detection rate is significantly higher than we would expect for a sample of optically selected ellipticals with the same redshift range. We find 40% of our sample have infrared luminosities of at least $10^9\ L_\odot$, as opposed to about 8% of normal ellipticals.

2. In spite of conclusion 1, we do not see a significant correlation between infrared and *total* radio emission within our sample itself. There is, however, a weak connection between the 60 μm flux density and the radio emission from the galactic cores of the radio sources.

3. The three most infrared-luminous galaxies in our sample are the three galaxies that are listed as "peculiar" by Zwicky. In these galaxies the physical conditions are probably similar to those in spiral galaxies or Centaurus A.

4. The infrared properties of the sample galaxies are inhomogeneous. While some galaxies, such as peculiars, have infrared/radio ratios and 25 μm/60 μm colors characteristic of star-forming galaxies, others contain active nuclei.

5. Most radio galaxy nuclei show much more radio emission as compared to infrared emission than do Seyfert galaxies, even when the emission from the extended lobes has been discounted. Either the central engines of radio galaxies produce radio power without ultraviolet power, or the radio emission of Seyfert galaxies is suppressed, or there is too little dust in radio galaxies to absorb the nuclear ultraviolet radiation.

6. A reconsideration of the available infrared data on nearby Shapley-Ames galaxies provides confirmation of our Paper I conclusion that the 10–12 μm emission is extended in normal (not radio-selected) elliptical galaxies. This result indicates that the 10 μm emission in such galaxies arises either from circumstellar dust shells around evolved stars or from PAH–like grains, rather than from nuclear activity.

We would like to thank Ron Koehler, Charlie Kaminski, David Griep, and John Hamilton for their nights of careful support on the IRTF. We are also grateful to Dolores Walther for assistance on the IRTF. Walter Rice and the Data Management Team at IPAC provided excellent support and quick turnaround despite a constant barrage of requests for data. Jim Heasley and John Peacock provided useful suggestions on statistical tests. We thank John Tonry for the MONGO plotting package, Julia Riley and Paul Alexander for discussions, and an anonymous referee for useful suggestions. C. D. I. is grateful for support provided by the SERC under a NATO Fellowship at the Institute of Astronomy, Hawaii, and acknowledges the support of a Caltech Weingart Fellowship. E. E. B. and C. G. W.-W. were supported under NSF grants AST 84-18197 and 86-15684. C. G. W.-W. also gratefully acknowledges support from the Royal Society and from Trinity College during sabbatical leave in Cambridge. This research was supported in part under the *IRAS* extended mission program by JPL contract 95782.

REFERENCES

Bally, J., and Thronson, H. A. 1989, *A.J.*, **97**, 69.
Becklin, E. E., Tokunaga, A. T., and Wynn-Williams, C. G. 1982, *Ap. J.*, **263**, 624.
Bridle, A. H., Davis, M. M., Fomalont, E. B., Willis, A. G., and Strom, R. G. 1979, *Ap. J.* (*Letters*), **228**, L9.
Bridle, A. H., Fomalont, E. B., and Cornwell, T. J. 1981, *A.J.*, **86**, 1294.
Cataloged Galaxies and Quasars Observed in the IRAS Survey, Verson 2. 1989, prepared by C. J. Lonsdale, G. Helou, J. Good, and W. Rice (Pasadena: JPL).
Colla, G., Fanti, C., Fanti, R., Gioia, I., Lari, C., Lequeux, J., Lucas, R., and Ulrich, M.-H. 1975*a*, *Astr. Ap.*, **38**, 209.
———. 1975*b*, *Astr. Ap. Suppl.*, **20**, 1.
de Grijp, M. H. K., Miley, G. K., and Lub, J. 1987, *Astr. Ap. Suppl.*, **70**, 95.
de Grijp, M. H. K., Miley, G. K., Lub, J., and de Jong, T. 1985, *Nature*, **314**, 240.
de Vaucouleurs, G., de Vaucouleurs, A., and Corwin, H. G. 1976, *Second Reference Catalog of Bright Galaxies* (Austin: University of Texas Press).
Edelson, R. A. 1987, *Ap. J.*, **313**, 651.
Edelson, R. A., Malkan, M. A., and Rieke, G. H. 1987, *Ap. J.*, **321**, 233.
Eilek, J. A., Burns, J. O., O'Dea, C. P., and Owen, F. N. 1984, *Ap. J.*, **278**, 37.
Ekers, R. D., Fanti, R., Lari, C., and Parma, P. 1978, *Nature*, **278**, 588.
———. 1981, *Astr. Ap.*, **101**, 194.
Elvis, M., Willner, S. P., Fabbiano, G., Carleton, N. P., Lawrence, A., and Ward, M. 1984, *Ap. J.*, **280**, 574.
Fanti, C., Fanti, R., de Ruiter, H. R., and Parma, P. 1986, *Astr. Ap. Suppl.*, **65**, 145.
———. 1987, *Astr. Ap. Suppl.*, **69**, 57.
Fanti, R., Lari, C., Parma, P., Bridle, A. H., Ekers, R. D., and Fomalont, E. B. 1982, *Astr. Ap.*, **110**, 169.
Feretti, L., and Giovannini, G. 1985, *Astr. Ap.*, **147**, L13.
Fomalont, E. B., Bridle, A. H., Willis, A. G., and Perley, R. A. 1980, *Ap. J.*, **237**, 418.
Gezari, D. Y., Schmitz, M., and Mead, J. M. 1987, *Catalog of Infrared Observations*. NASA Reference Pub. 1196 (Washington, DC: NASA).
Golombek, D., Miley, G. K., and Neugebauer, G. 1988, *A.J.*, **95**, 26.
Heckman, T. M., Lebofsky, M. J., Rieke, G. H., and van Breugel, W. 1983, *Ap. J.*, **272**, 400.
Helou, G. 1986, *Ap. J.* (*Letters*), **311**, L33.
Helou, G., Soifer, B. T., and Rowan-Robinson, M. 1985, *Ap. J.* (*Letters*), **298**, L7.
Impey, C. D., and Neugebauer, G. 1988, *A. J.*, **95**, 307.
Impey, C. D., Wynn-Williams, C. G., and Becklin, E. E. 1986, *Ap. J.*, **309**, 572 (Paper I).
IRAS Catalogs and Atlases: Explanatory Supplement. 1988, ed. C. A. Beichman, G. Neugebauer, H. J., Habing, P. E. Clegg, and T. J. Chester (Washington, D.C.: US Government Printing Office).
IRAS Point Source Catalog, Version 2. 1988, prepared by G. Helou and D. Walker (Washington DC: US Government Printing Office).
Joy, M., Lester, D. F., Harvey, P. M., and Ellis, H. B. 1988, *Ap. J.*, **326**, 662.
Jura, M. 1986, *Ap. J.*, **306**, 483.
Jura, M., Kim, D. W., Knapp, G. R., and Guhathakurta, P, 1987, *Ap. J.* (*Letters*), **312**, L11.
Knapp, G. R., Guhathakurta, P., Kim, D.-W., and Jura, M. 1989, *Ap. J. Suppl.*, **70**, 329.
Kuhr, H., Witzel, A., Pauliny-Toth, I. I. K., and Nauber, A. 1981, *Astr. Ap. Suppl.*, **45**, 367.
Lilly, S. J., Longair, M. S., and Miller, L. 1985, *M.N.R.A.S.*, **214**, 109.
Marston, A. P., and Dickens, R. J. 1988, *Astr. Ap.*, **193**, 27.
O'Dea, C. P. and Owen, F. N. 1985, *A.J.*, **90**, 927.
Parma, P., de Ruiter, H. R., Fanti, C., and Fanti, R. 1986, *Astr. Ap. Suppl.*, **64**, 135.
Perley, R. A., Willis, A. G., and Scott, J. S. 1979, *Nature*, **281**, 437.
Puschell, J. J. 1981, *Ap. J.*, **247**, 48.
Rieke, G. H., and Lebofsky, M. J., 1986, *Ap. J.*, **304**, 326.
Rieke, G. H., Lebofsky, M. J., and Kemp, J. C. 1982, *Ap. J.* (*Letters*), **252**, L53.
Schilizzi, R. T., Fanti, C., Fanti, R., and Parma, P. 1983, *Astr. Ap.*, **126**, 412.
Soifer, B. T., Sanders, D. B., Neugebauer, G., Danielson, G. E., Lonsdale, C. J., Madore, B. F., and Persson, S. E. 1986, *Ap. J.* (*Letters*), **303**, L41.
Ulvestad, J. S., and Wilson, A. S. 1984, *Ap. J.*, **285**, 439.
van Breugel, W., Heckman, T., and Miley, G. 1984, *Ap. J.*, **276**, 79.
van den Bergh, S. 1970, *Pub. A.S.P.*, **82**, 1379.
Walsh, D. E. P., Knapp, G. R., Wrobel, J. M., and Kim, D.-W. 1989, *Ap. J.*, **337**, 209.
Wrobel, J. M., Neugebauer, G., and Miley, G. K. 1986, *Ap. J.* (*Letters*), **310**, L11.
Wunderlich, E., Klein, U., and Wielebinski, R. 1987, *Astr. Ap. Suppl.*, **69**, 487.
Young, E. T., Neugebauer, G., Kopan, E. L., Conrow, T. P., Rice, W. L., and Gregorich, D. T. 1988, *A Users Guide to IRAS Pointed Observation Products*, IPAC preprint PRE-008N.

E. E. BECKLIN: Department of Astronomy, UCLA, Los Angeles, CA 91103

C. D. IMPEY: Steward Observatory, University of Arizona, Tucson, AZ 85721

C. G. WYNN-WILLIAMS: Institute for Astronomy, 2680 Woodlawn Drive, Honolulu, HI 96822